European Journal of Mechanics B/Fluids 28 (2009) 619–629

Contents lists available at ScienceDirect

European Journal of Mechanics B/Fluids

journal homepage: www.elsevier.com/locate/ejmflu

Particle and bubble dynamics in a creeping flow

Yury A. Stepanyants [a,b,*], Guan H. Yeoh [a,c]

[a] Reactor Operations, Australian Nuclear Science and Technology Organisation (ANSTO), Lucas Heights, PMB 1, Menai (Sydney), NSW 2234, Australia
[b] Department of Mathematics and Computing, The University of Southern Queensland, Toowoomba, Australia
[c] School of Mechanical and Manufacturing Engineering, The University of New South Wales, Sydney, Australia

ARTICLE INFO

Article history:
Received 13 February 2009
Received in revised form
7 April 2009
Accepted 27 April 2009
Available online 9 May 2009

Keywords:
Creeping flow
Solid particle
Bubble
Viscous fluid
Small Reynolds number
Exact solution
Stokes drag
Memory-integral drag

ABSTRACT

Dynamics of a solid particle and non-deformable gaseous bubble in viscous fluid are studied analytically and numerically within the framework of creeping flow regime (flow at vanishingly small Reynolds numbers). Equations of motion for the particle and bubble include the consideration of the buoyancy force, Stokes drag force and memory-integral drag force. Exact analytical solutions are obtained and categorised in terms of inclusion (particle or bubble) density with respect to the density of a surrounding fluid. Through the analytical and numerical solutions, the dynamics of solid particle and air bubble in water have been found to behave differently especially at the early stages of motion, whereas some qualitative similarities exist in the long-term asymptotic.

1. Introduction

Over the years, there has been much development on the equation of motion for solid particles moving in a viscous fluid at small Reynolds numbers. In 1845, Stokes derived a formula for a drag force exerting on a *stationary* moving *solid* spherical particle in the limit of a *creeping flow*, i.e. for the flow of vanishingly small Reynolds number, $Re \to 0$ (the term "creeping flow" was actually introduced much later by Sy et al. [17]). Currently the well-known formula for the Stokes drag (SD) force $F = 6\pi\mu RV$ can be found in any textbook on hydrodynamics; the force is proportional to the molecular viscosity of a fluid μ, radius of a moving particle R, and particle velocity V. For small but finite $Re \ll 1$, Oseen later, in 1910 and 1913, obtained a correction to the Stokes formula, and a further correction to Oseen's solution was proposed by Proudman and Pearson in 1956 (for more details, see Section 20 of Chapter 2 in Landau and Lifshitz [12]).

In 1911, Hadamard, and independently, Rybczynski, obtained an expression which generalised Stokes formula for stationary moving spherical *liquid inclusions (drops)* in a viscous fluid (for more details, see Section 20 of Chapter 2 in Ref. [12] or Section 4.9 in Ref. [2]). A general formula for the drag force exerting on a drop of any density and viscosity reduces to the Stokes formula in a limit, when the drop viscosity is much greater than the viscosity of a surrounding fluid. In another limit, when the drop viscosity is negligibly small in comparison with the viscosity of surrounding fluid, the coefficient in the Stokes formula is altered to the value of 4 instead of 6, i.e. $F = 4\pi\mu RV$. In particular, this result is applicable to a stationary moving *air bubble* in water since the corresponding ratio of molecular viscosities of air to water is $\mu_a/\mu_w \approx 0.018$ and can, therefore, be treated as negligibly small. Hence, the drag force exerting on a bubble amounts two-thirds of the drag force exerting on a solid particle of the same radius.

For a *non-stationary* moving *solid* particle, Boussinesq in 1885 and Basset in 1888 derived, in addition to the SD force, a memory-integral drag (MID) force which is known nowadays as the Boussinesq–Basset drag (BBD) force (the corresponding expression is presented in the text below). The derivation of this force for the case of a solid particle moving in a quiescent fluid can be found in many textbooks (see, e.g., problem 7 of Section 24 in Ref. [12]). Ever since then, many other corrections to SD and BBD forces have been obtained for the case of a particle moving in fluid which in turn moves non-uniformly in space and non-stationary in time, e.g., the Faxen (1922) correction due to non-uniformity in the external fluid flow, Saffman (1965) lift force due to external shear flow and

* Corresponding author. Department of Mathematics and Computing, The University of Southern Queensland, Toowoomba, Australia.
E-mail address: yuas50@gmail.com (Y.A. Stepanyants).

0997-7546/$ – see front matter
doi:10.1016/j.euromechflu.2009.04.004

particle rotation in the course of motion (an extension of Saffman's results to the drop of arbitrary internal viscosity has been established by Ref. [13]), etc. Historical details and analogy for a particle motion in a viscous fluid and heat transfer processes can be found in the review paper by Michaelides [15].

The most recent comprehensive revision of the equation of drop motion, that includes gaseous bubbles and solid particles, has been undertaken by Lovalenty and Brady [14] in 1993. In Oseen's approximation of small but finite *Re*, an equation of motion for a fluid drop of arbitrary density and viscosity in a surrounding viscous fluid was derived when both the drop and fluid move with transient velocities provided that the Reynolds number for the drop remains small. The equation derived contains rather complex general expression for the total drag force exerting on the drop. For a spherical inclusion (particle or bubble) in the limit of Stokes approximation, i.e. up to terms of the order of $O(Re)$ only, the equation of motion contains two components of the drag force, the SD force with the Hadamard–Rybczynski drag coefficient and the MID force with a complex integral kernel (the BBD force is treated as the particular case of a general MID force which is applicable to solid particles only). The expression for the integral kernel in a general case of a drop of arbitrary viscosity and density moving in a quiescent viscous fluid was derived for the first time by Gorodtsov [9] as early as 1975 (its generalisation to a drop moving in an inhomogeneous transient flow was later appeared in the paper by Parshikova [16], 1982). An expression similar to Gorodtsov's formula was also derived in the book by Kim and Karrila [10], however due to regrettable error, they arrive at a formula in which the kinematic viscosities of fluids inside and outside the drop were implicitly assumed to be equal. The error was corrected in the papers by Lovalenty and Brady [14] and Galindo and Gerbeth [8] who independently rediscovered Gorodtsov's formula and noticed that Kim and Karrila's formula is valid only in two limiting cases: (i) solid particle whose viscosity is infinitely large with respect to ambient fluid viscosity and (ii) inviscid drop (e.g., a drop of superfluid in the viscous fluid or approximately air bubble in water).

Analysis of the formula for the integral kernel reveals some interesting features [8] (early similar analysis was undertaken by Yang and Leal [21] on the basis of incorrect results of Kim and Karrila [10]). In particular, as shown by Galindo and Gerbeth [8], MID force can be negative at some relationship between the density ratio of internal to external liquid and corresponding viscosity ratio. This means that the MID force may act as an acceleration force at certain circumstances and contrary to the SD force, which is always dissipative force, can add kinetic energy to the inclusion, at least momentarily [11]. However, this is not related to the two aforementioned cases of rigid particle and zero viscosity drop moving in the quiescent fluid: in both these cases the BBD and MID forces are positive and monotonically decreasing [8,21].

A general expression for the integral kernel is fairly complex; it is only known in the algebraic form in the Fourier-transform domain. However, it simplifies and takes rather simple form in two particular cases mentioned above, when the internal drop viscosity is much greater than the viscosity of surrounding fluid (the case of solid particle) and when it is negligibly small (the case relevant to an air bubble in water). In both these cases the total drag force is essentially positive and consists of the SD force (with different numerical coefficients for the solid particle and air bubble) and MID force, whose analytical expression is different for these two inclusions (they are presented below).

Owing to the memory integral term in the equation of the drop motion, its solution is not trivial whether they are solved analytically or numerically even in the limiting cases of particle or bubble motion. Nevertheless, in few cases analytical solutions were obtained by means of Laplace transform method [3,4] and fractional calculus technique [6,11]. The cases studied are related to particle and bubble motion in a solid-body rotation flow [3,4,6] and in linear solenoidal velocity field [11]. Results obtained in those papers are in a reasonable agreement with experimental data [3,4] and general physical insights [6,11]. In few in number papers, numerical solutions of the equation of particle motion were constructed for some particular cases [18,7,19] of particle motion in given velocity fields (we leave aside the papers where drop motions in viscous fluids were studied by numerical simulations of the Navier–Stokes equation).

In the meantime, analysis of solutions of the governing equations describing particle and bubble dynamics in quiescent viscous fluid has not been performed thus far. Such analysis conducted even within the framework of reasonably simplified model of creeping flow is important for the understanding of peculiarities of motion of inclusions and physical insight formation because, as has been mentioned above, an action of BBD and, in general, MID forces may be fairly nontrivial and unexpected in general. In this paper, we examine a motion of the solid particle and gaseous bubble in quiescent viscous fluid through the exact solutions to the equations of their motion in the creeping flow regime. Detailed solutions categorisation is presented for a solid particle depending on its density. Peculiarities of motions are compared and discussed for the solid particle of negligibly small density and gaseous bubble.

For the sake of simplicity, both the particle and bubble are assumed to be spherical in shape. The sphericity of a bubble is guaranteed if the surface tension σ is sufficiently large, $\sigma \gg \rho_w g R^2$ (see, e.g., problem 2 of Section 20 in Ref. [12]), or the bubble radius is sufficiently small, (this corresponds to small Bond numbers, $Bo \equiv \rho_w g R^2/\sigma \ll 1$). Substituting $\sigma = 7.23 \times 10^{-2}$ N/m at the interface of air and clean water of the temperature $T = 20\,^\circ$C and corresponding water density $\rho_w = 998.2$ kg/m^3, one obtains $R_{cap} \approx 2.7$ mm. However, it is well known that bubbles in the limit of creeping flow remain spherical even though their radii enlarge such that the surface tension becomes negligible [2,5].

The creeping flow approximation exploited in this paper formally presumes that the Reynolds number is vanishingly small ($Re \to 0$). However, as shown in Batchelor [2] (see Fig. 4.9.2 in his book and the concomitant text there) and widely adopted by other researchers, satisfactory results for the description of motion of a rigid sphere may be obtained beyond the formal range of theory validity up to *Re* of the order of unity. In the meantime, there is a temporal limitation on the application of a creeping flow approximation for transient motions [14]: $t < t_{lim} \equiv \rho R^2/\mu$, where ρ and μ stands for the density and dynamic viscosity of external fluid, whereas R is the radius of a moving body. The results obtained in this paper are valid only within the framework of both these limitations $Re < 1$ and $t < t_{lim}$. Additional discussion on these limitations in conjunction with the results obtained is given in Section 4.

It is envisaged that theoretical results obtained in this paper can be employed for the description of various processes occurring in the industry, engineering and nature, e.g. in the pharmaceutical and perfumery industry dealing with aerosols and powder production, in problems of cavitation and nucleate boiling dealing with the dynamics of micro-bubbles, in the study of dust transport in the atmosphere and fine sediment transport in oceans, seas and lakes.

2. Motion of a solid spherical particle in a viscous fluid

2.1. Equation of motion and its exact solutions

Consider a solid spherical particle of a radius R travelling in a quiescent viscous fluid under the combined action of the gravity and buoyancy (Archimedean) forces. Corresponding equation of motion in the creeping flow regime is [12,14]:

$$\left(r+\frac{1}{2}\right)\frac{\mathrm{d}^2z}{\mathrm{d}t^2}=(1-r)g-\frac{9}{2}\frac{\nu_\mathrm{f}}{R^2}\frac{\mathrm{d}z}{\mathrm{d}t}-\frac{9}{2}\frac{1}{R}\sqrt{\frac{\nu_\mathrm{f}}{\pi}}\int_{-\infty}^{t}\frac{\mathrm{d}^2z(\tau)}{\mathrm{d}\tau^2}\frac{\mathrm{d}\tau}{\sqrt{t-\tau}}, \tag{1}$$

where z is the particle's vertical coordinate with the axis z directed upwards; $r\equiv\rho_\mathrm{p}/\rho_\mathrm{f}$ is the ratio of particle to fluid density; g is the acceleration due to gravity, and $\nu_\mathrm{f}\equiv\mu_\mathrm{f}/\rho_\mathrm{f}$ is the kinematic viscosity of a fluid. From the above equation, the second term in the right hand side describes the quasi-stationary SD force, while the last integral term describes the well-known BBD force. Added mass effect for the spherical particle is accounted for through the coefficient 1/2 within the bracket in the left hand side of the equation. We assume that the particle being at rest commences with an instantaneous motion at $t=0$ with an initial velocity V_0, i.e. its velocity experiences a sudden jump from zero to V_0 and then, varies in accordance with the equation of motion (1). Thus, the particle velocity, including the initial jump, can be expressed through the unit Heaviside function [20] $\mathrm{H}(t)$: $(\mathrm{d}z/\mathrm{d}t)_\mathrm{tot}=\mathrm{H}(t)(\mathrm{d}z/\mathrm{d}t)_\mathrm{pos}$, where $(\mathrm{d}z/\mathrm{d}t)_\mathrm{tot}$ is the velocity at any instant of time, whereas $(\mathrm{d}z/\mathrm{d}t)_\mathrm{pos}$ relates to the velocity at positive times only. Correspondingly, the acceleration is $(\mathrm{d}^2z/\mathrm{d}t^2)_\mathrm{tot}=\delta(t)(\mathrm{d}z/\mathrm{d}t)_\mathrm{pos}+\mathrm{H}(t)(\mathrm{d}^2z/\mathrm{d}t^2)_\mathrm{pos}$, where $\delta(t)\equiv\mathrm{dH}(t)/\mathrm{d}t$ is the Dirac delta-function. Taking into consideration the effect of the Dirac delta-function under the integral, Eq. (1) for $t>0$ can be presented in the form (the index "pos" has been omitted):

$$\left(r+\frac{1}{2}\right)\frac{\mathrm{d}^2z}{\mathrm{d}t^2}=(1-r)g-\frac{9\nu_\mathrm{f}}{2R^2}\left[\frac{\mathrm{d}z}{\mathrm{d}t}+\frac{RV_0}{\sqrt{\pi\nu_\mathrm{f}t}}+\frac{R}{\sqrt{\pi\nu_\mathrm{f}}}\int_{0+}^{t}\frac{\mathrm{d}^2z(\tau)}{\mathrm{d}\tau^2}\frac{\mathrm{d}\tau}{\sqrt{t-\tau}}\right]. \tag{2}$$

The equation of motion can be conveniently expressed in dimensionless form by introducing the following normalised variables and parameters G and υ_0:

$$\zeta=\frac{z}{R},\quad \theta=\frac{9\nu_\mathrm{f}}{R^2}t,\quad G(r)=\frac{2}{81}\frac{1-r}{1+2r}\frac{gR^3}{\nu_\mathrm{f}^2},\quad \upsilon_0=\frac{V_0R}{9\nu_f}. \tag{3}$$

Eq. (2) is thus given as:

$$\frac{\mathrm{d}^2\zeta}{\mathrm{d}\theta^2}=G(r)-\frac{1}{1+2r}\left[\frac{\mathrm{d}\zeta}{\mathrm{d}\theta}+\frac{3\upsilon_0}{\sqrt{\pi\theta}}+\frac{3}{\sqrt{\pi}}\int_{0+}^{\theta}\frac{\mathrm{d}^2\zeta(\tau)}{\mathrm{d}\vartheta^2}\frac{\mathrm{d}\vartheta}{\sqrt{\theta-\vartheta}}\right]. \tag{4}$$

Note that the condition of validity of this equation in consistency with the creeping flow regime (see above), $Re\le 1$, reduces to the requirement $\upsilon(\theta)\le 1/9$, where $\upsilon(\theta)=\mathrm{d}\zeta/\mathrm{d}\theta$ is the normalised particle velocity.

Eq. (4) is solved by the Laplace transform method. Application of the Laplace transformation with the parameter s yields the equation for the velocity Laplace image $\tilde{\upsilon}(s)$:

$$s\tilde{\upsilon}(s)-\upsilon_0=\frac{G(r)}{s}-\frac{1}{1+2r}\left[\tilde{\upsilon}(s)+\frac{3\upsilon_0}{\sqrt{s}}+3\frac{s\tilde{\upsilon}(s)-\upsilon_0}{\sqrt{s}}\right], \tag{5}$$

The solution to this equation is:

$$\tilde{\upsilon}(s)=\upsilon_0\frac{(s+a)+c-\left(3\sqrt{s}/(1+2r)\right)}{(s+a)^2\pm b^2}+G(r)\frac{(s+a)+c-\left(3\sqrt{s}/(1+2r)\right)}{s\left[(s+a)^2\pm b^2\right]}. \tag{6}$$

when $r<5/8$, the denominator in Eq. (6) is given by $(s+a)^2-b^2$. Otherwise, when $r>5/8$, the denominator is $(s+a)^2+b^2$. The parameters a, b and c are given by:

$$a=\frac{4r-7}{2(2r+1)^2};\quad b=\frac{3}{2}\frac{\sqrt{|8r-5|}}{(2r+1)^2};\quad c=\frac{9}{2(2r+1)^2} \tag{7}$$

After performing the Laplace inversion on Eq. (6), two distinct components can be ascertained in the complete solution $\upsilon(\theta)=\upsilon_\upsilon(\theta)+\upsilon_\mathrm{G}(\theta)$, where the first component, $\upsilon_\upsilon(\theta)$, is caused by the influence of nonzero initial condition, while the second component, $\upsilon_\mathrm{G}(\theta)$, is caused by the influence of nonzero gravity/buoyancy effect.

Representation of the analytical solution in the real space is significantly influenced by the density ratio r. Depending on the sign in the denominators of Eq. (6), there are two ranges of possible solutions: (i) $0\le r<5/8$ – "light particles range" and (ii) $r>5/8$ – "heavy particles range". These two ranges are distinguished by the "transitional" value of particle density $r=5/8$ when $b=0$.

In the case of relatively light particle, the exact solution of Eq. (4) subject to the initial condition $\upsilon(0)=\upsilon_0$ is presented in the real space through the two abovementioned velocity components (designated by the additional index l):

$$\upsilon_{\upsilon\mathrm{l}}(\theta)=\frac{\upsilon_0}{2\sqrt{5-8r}}\left\{\left(3+\sqrt{5-8r}\right)\exp[-(a-b)\theta]\mathrm{erfc}\left[\sqrt{-(a-b)\theta}\right]-\left(3-\sqrt{5-8r}\right)\exp[-(a+b)\theta]\mathrm{erfc}\left[\sqrt{-(a+b)\theta}\right]\right\}, \tag{8a}$$

$$\upsilon_{\mathrm{Gl}}(\theta)=G(r)(2r+1)\left\{1+\frac{1}{2\sqrt{5-8r}}\times\left[\left(3-\sqrt{5-8r}\right)\exp[-(a-b)\theta]\mathrm{erfc}\left[\sqrt{-(a-b)\theta}\right]-\left(3+\sqrt{5-8r}\right)\exp[-(a+b)\theta]\mathrm{erfc}\left[\sqrt{-(a+b)\theta}\right]\right]\right\}, \tag{8b}$$

where $\mathrm{erfc}(x)=1-\mathrm{erf}(x)$ is the complimentary error function [20].

In the transitional case of $r=5/8$ when, $a=-4/9$, $b=0$ and $c=8/9$, the components of the exact solution (designated by the additional index t) are:

$$\upsilon_{\upsilon\mathrm{t}}(\theta)=\upsilon_0\left[\left(1+\frac{8}{9}\theta\right)\mathrm{e}^{4\theta/9}\mathrm{erfc}\left(\sqrt{\frac{4}{9}\theta}\right)-\frac{4}{3}\sqrt{\frac{\theta}{\pi}}\right], \tag{9a}$$

$$\upsilon_{\mathrm{Gt}}(\theta)=\frac{9}{4}G(r)\left[1-\left(1-\frac{8}{9}\theta\right)\mathrm{e}^{4\theta/9}\mathrm{erfc}\left(\sqrt{\frac{4}{9}\theta}\right)-\frac{4}{3}\sqrt{\frac{\theta}{\pi}}\right]. \tag{9b}$$

And in the case of a relatively heavy particle the components of the exact solution (designated by the additional index h) are:

$$\upsilon_{\upsilon\mathrm{h}}(\theta)=\upsilon_0\left\{\left[\cos(b\theta)+\frac{3}{\sqrt{8r-5}}\sin(b\theta)\right]\mathrm{e}^{-a\theta}-\frac{3}{2r+1}\left[I\cos(\theta,a,b)-\frac{4r-7}{3\sqrt{8r-5}}I\sin(\theta,a,b)\right]\right\}, \tag{10a}$$

$$\upsilon_{\mathrm{Gh}}(\theta)=\frac{G(r)}{b}\left\{\left(1-\frac{1}{2}\frac{4r-7}{2r+1}\mathrm{e}^{-a\theta}\right)\sin(b\theta)+\frac{3}{2}\frac{\sqrt{8r-5}}{2r+1}\times\left[1-\cos(b\theta)\mathrm{e}^{-a\theta}\right]-\frac{3}{2r+1}I\sin(\theta,a,b)\right\}. \tag{10b}$$

Functions $I\cos(\theta, a, b)$ and $I\sin(\theta, a, b)$ can be presented either through the integrals or error function of complex argument [20]:

$$I\cos(\theta,a,b) = \frac{1}{\sqrt{\pi}}\int_0^\theta \frac{\exp(-at)\cos(bt)}{\sqrt{\theta-t}}\,\mathrm{d}t = \mathrm{Re}\left\{\frac{\exp[-(a-ib)\theta]\mathrm{erf}\left[\sqrt{-(a-ib)\theta}\right]}{\sqrt{-(a-ib)}}\right\}, \quad (11a)$$

$$I\sin(\theta,a,b) = \frac{1}{\sqrt{\pi}}\int_0^\theta \frac{\exp(-at)\sin(bt)}{\sqrt{\theta-t}}\,\mathrm{d}t = \mathrm{Im}\left\{\frac{\exp[-(a-ib)\theta]\mathrm{erf}\left[\sqrt{-(a-ib)\theta}\right]}{\sqrt{-(a-ib)}}\right\}, \quad (11b)$$

The integrals in Eq. (11) can be readily calculated numerically, whereas their more complex representation in terms of the error function allows the convenient provision of determining the integral asymptotes.

Note that the solution for a very heavy particle with $r \gg 1$ significantly simplifies in the asymptotic limit $r \to \infty$. In this limiting case the viscosity of external fluid does not affect the motion of a very heavy particle and the solution can be readily obtained directly from Eq. (4) with $G(\infty) = 2gR^3/(81\nu_f^2)$: $\zeta(\theta) = \zeta_0 + v_0\theta + G(\infty)\theta^2/2$, $v(\theta) = v_0 + G(\infty)\theta$.

In the particular case of $r = 7/4$ when $a = 0$, $b = 2/9$ and $c = 2/9$, Eq. (10) degenerates and becomes:

$$v_{hs}(\theta) = v_0\left\{\cos\left(\frac{2}{9}\theta\right)\left[1-2C\left(\frac{2}{3}\sqrt{\frac{\theta}{\pi}}\right)\right] + \sin\left(\frac{2}{9}\theta\right)\times\left[1-2S\left(\frac{2}{3}\sqrt{\frac{\theta}{\pi}}\right)\right]\right\} + \frac{9}{2}G(r)\left\{1-\cos\left(\frac{2}{9}\theta\right)\times\left[1-2S\left(\frac{2}{3}\sqrt{\frac{\theta}{\pi}}\right)\right] + \sin\left(\frac{2}{9}\theta\right)\left[1-2C\left(\frac{2}{3}\sqrt{\frac{\theta}{\pi}}\right)\right]\right\}, \quad (12)$$

where the subscript "*hs*" designates a special case of a heavy particle, $C(x) = \int_0^x \cos(\pi\xi^2/2)\mathrm{d}\xi$ and $S(x) = \int_0^x \sin(\pi\xi^2/2)\mathrm{d}\xi$ are the Fresnel's integrals [20].

All the above solutions obtained can be compared with the solution of Eq. (4) when only the SD force is taken into account, i.e. only the first term in the square brackets of Eq. (4). In this case the exact solution becomes:

$$v_{St}(\theta) = v_0\exp\left(-\frac{\theta}{2r+1}\right) + (2r+1)G(r)\left[1-\exp\left(-\frac{\theta}{2r+1}\right)\right]. \quad (13)$$

2.2. Particle motion in a fluid without gravity

Consider first the case when a particle begins with a sudden motion of an initial velocity v_0 in the quiescent fluid without presence of gravity. In the absence of gravity the parameter $G(r) = 0$, this can be realised either due to $g = 0$ or $r = 1$ (see Eq. (3)). Let us consider the former case, namely $g = 0$, by letting r being the free parameter.

If the BBD force can be formally neglected, then solution (13) demonstrates that the particle velocity decays exponentially in time $v_{St}(\theta) = v_0\exp(-(\theta/(2r+1)))$, whereas due to the effect of BBD force, particle velocity asymptotically, for large θ, decays much slower, in a power-type dependence according to $v(\theta) \sim \theta^{-3/2}$. The coefficient of proportionality in this formula depends on the density ratio. For all cases as described by Eqs. (8a)–(10a) and the first term of Eq. (12), the universal asymptotic formula is thus given by

$$v_{as}(\theta) = \frac{3}{2}\frac{2r+1}{\sqrt{\pi}}v_0\theta^{-3/2} \quad (14)$$

Fig. 1 presents the solutions to Eqs. (8)–(10) and (12) plotted in a logarithmic scale for different values of density ratio. The following values of the parameter r have been chosen: $r = 0$ – very light solid particle in the dense liquid; $r = 5/8$ – light particle of the transitional density (which corresponds to $b = 0$); $r = 1$ – solid particle of the same density as the surrounding fluid; $r = 7/4$ – special case of heavy particle corresponding to $a = 0$; and $r = 2.7$ – aluminium particle in water (the case of practical interest that could be experienced, for instance, in an open pool nuclear reactor). In addition to the analytical solutions, predicted results obtained by means of numerical solution of the Newtonian Eq. (4) by the Runge–Kutta method are also presented for two particular cases: $r = 0$ and $r = 2.7$. It should be noted that the numerical solution of Eq. (4) is rather cumbersome; it is time consuming, requires significant computational resources and provides reasonable results only in a limiting time interval which depends on the density ratio r (cf. analytical and numerical data shown around lines 1 and 5 in Fig. 1).

As depicted in Fig. 1, the behaviour of all the curves is qualitatively similar in spite of their different analytical considerations. Even in the limiting case of a very light solid particle in a dense fluid, $r = 0$, the dependence of particle velocity on time is well described by Eq. (8) (this case of a *solid particle* with $r = 0$ should not be confused with the bubble of the same density (see below); for a solid particle the internal viscosity is formally infinite, whereas for the bubble we assume that the internal viscosity is negligibly small).

Another interesting case worth mentioning is the behaviour of solid particle of the same density as the surrounding fluid, $r = 1$ (line 3 in Fig. 1). In this case the dimensionless parameter $G(1) = 0$ even when $g \neq 0$ due to the effect of the gravity force compensating the buoyancy force. Such situation can be realised, in particular, when a spherical particle of heavy water (D_2O) ice travelling in

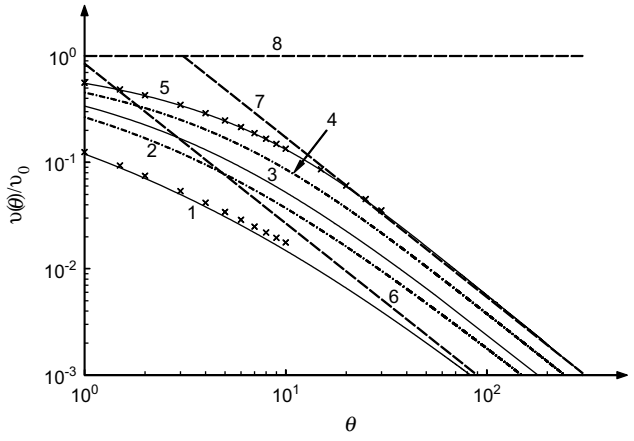

Fig. 1. Normalised particle velocity as a function of time in dimensionless variables for different values of particle to fluid density ratio. Line 1, $r = 0$; line 2, $r = 5/8$; line 3, $r = 1$; line 4, $r = 7/4$; line 5, $r = 2.7$. Dashed lines 6 and 7 show the asymptotic dependence (14) for the cases $r = 0$ (line 6) and $r = 2.7$ (line 7), whereas dashed line 8 shows the asymptotic dependence for a very heavy particle with $r = \infty$. Crosses represent results of direct numerical calculations undertaken within the framework of Eq. (4) for $r = 0$ and $r = 2.7$.

usual light water within the temperature range $0\,^{\circ}\mathrm{C} < T < 4\,^{\circ}\mathrm{C}$, i.e. above the melting point of light water but below the melting point of heavy water.

Note that the asymptotic power-type dependence (14) onsets later, if the parameter r increases. In particular, when $r \to \infty$ the transition to the power-type dependence moves away to the infinity so that v/v_0 goes to unity for all finite θ. This illustrates by horizontal line 8 in Fig. 1.

Knowledge of particle velocity as a function of time allows the traversed path to be determined via simple integration of Eqs. (8)–(10) and (12). The corresponding formulae subject to zero initial condition for the particle coordinate are:

(a) "light particle", $r < 5/8$,

$$\zeta_{vl}(\theta) = v_0(2r+1)\left\{1+\frac{1}{2\sqrt{5-8r}}\left(\left[\left(3-\sqrt{5-8r}\right)e^{\Theta_+}\left(\sqrt{\Theta_+}\right)\right.\right.\right.$$
$$\left.\left.\left.-\left(3+\sqrt{5-8r}\right)e^{\Theta_-}\left(\sqrt{\Theta_-}\right)\right]\right)\right\}, \qquad (15)$$

where $\Theta_\pm = ((3\pm\sqrt{5-8r})/(2r+1))^2(\theta/4)$;

(b) particle of a transitional density, $r = 5/8$,

$$\zeta_{vt}(\theta) = \frac{9}{4}v_0\left[1-\frac{4}{3}\sqrt{\frac{\theta}{\pi}}-\left(1-\frac{8}{9}\theta\right)e^{4\theta/9}\left(\sqrt{\frac{4}{9}\theta}\right)\right]; \qquad (16)$$

(c) "heavy particle", $r > 5/8$,

$$\zeta_{vh}(\theta) = v_0(2r+1)\left\{1-e^{-a\theta}\left[\cos(b\theta)-\frac{3}{\sqrt{8r-5}}\sin(b\theta)\right]\right.$$
$$\left.-\frac{2}{\sqrt{8r-5}}I\sin(\theta,a,b)\right\}; \qquad (17)$$

(d) special case of heavy particle, $r = 7/4$,

$$\zeta_{vhs}(\theta) = \frac{9}{2}v_0\left\{1+\sin\left(\frac{2}{9}\theta\right)\left[1-2C\left(\frac{2}{3}\sqrt{\frac{\theta}{\pi}}\right)\right]-\cos\left(\frac{2}{9}\theta\right)\right.$$
$$\left.\times\left[1-2S\left(\frac{2}{3}\sqrt{\frac{\theta}{\pi}}\right)\right]\right\} \qquad (18)$$

These solutions can also be compared with the solution of Eq. (4) when only the SD force is taken into account and the BBD force is neglected; the exact solution in this case is:

$$\zeta_{vSt}(\theta) = (2r+1)v_0\left[1-\exp\left(-\frac{\theta}{2r+1}\right)\right]. \qquad (19)$$

In all cases, the maximal traversed path depends on r and is equal to $\zeta_{max} = (2r+1)v_0$ (in the dimensional variables this gives $z_{max} = (2\rho_p/\rho_f + 1)V_0R^2/9\nu_f$). However, in the case when the only SD force is taken into account, the particle comes to the rest relatively quickly for the characteristic time $\theta_c = 2r+1$. In all other cases with the BBD force included, the particle comes to the final state for the infinite time in accordance with the following asymptotic formula:

$$\zeta_{vas}(\theta) = (2r+1)v_0\left(1-\frac{3}{\sqrt{\pi\theta}}\right). \qquad (20)$$

Fig. 2 illustrates the dependences of the normalised traversed path $\zeta(\theta)/\zeta_{max}$ as a function of time as described by Eqs. (15)–(19); the asymptotic dependence of Eq. (20) is also shown in the figure by the dashed line. All curves in normalised variables converge initially to the asymptotic dependence of Eq. (20) in a relatively short time of the order of θ_c. This dependence thus plays a role of an *intermediate asymptotic* [1] for all other dependences, while the final asymptotic state is the maximal traversed path shown in Fig. 2 by the horizontal dotted line. Eventually, the dependence (20) asymptotically approaches the final state for infinite time.

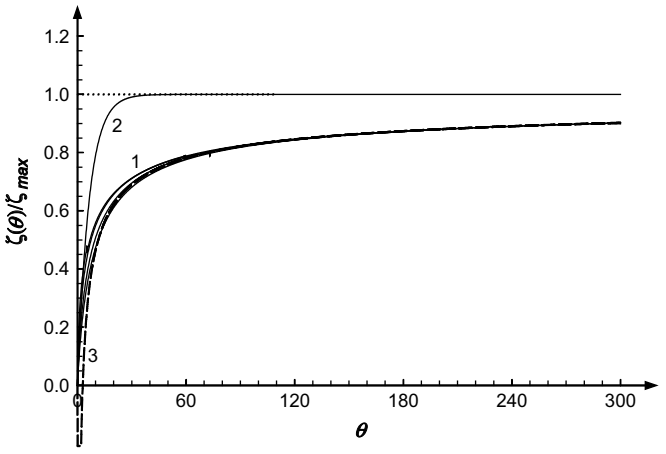

Fig. 2. Normalised traversed path as a function of time as described by Eqs. (15)–(19) for different values of particle to fluid density ratio. Line 1 corresponds to $r = 0$, and all other lines below it correspond consecutively to $r = 5/8$; $r = 7/4$; and $r = 2.7$. Line 2 shows the dependence (19) when the only SD force is taken into account, and dashed line 3 shows the asymptotic dependence (20) for the case $r = 2.7$.

2.3. Particle motion in a homogeneous fluid under the influence of gravity and buoyancy forces

Consider now the particle motion in a homogeneous viscous fluid when the gravity and buoyancy forces are taken into account. Equations (8)–(10) and (12) show that the solutions eventually reach the *terminal velocity* $v_{pt} = (2r+1)G(r)$, independently of the initial velocity. The asymptotic approach to the terminal velocity is rather slow, $\sim\theta^{-1/2}$, in contrast to the asymptotic decay of the v_v-component, $v_v(\theta) \sim \theta^{-3/2}$ (see Eq. (14)). The asymptotic dependence of v_G-component is given by the formula similar to Eq. (20):

$$v_{Gas}(\theta) = G(r)(2r+1)\left(1-\frac{3}{\sqrt{\pi\theta}}\right) \qquad (21)$$

Consistent with the condition of the creeping flow regime, v_{pt} must not be greater than 1/9 (see text after Eq. (4)). This therefore leads to the restriction on the particle radius which can be expressed in dimensional variables according to:

$$R \le \sqrt[3]{\frac{9\nu_f^2}{2g\left|1-\rho_p/\rho_f\right|}} \qquad (22)$$

To analyse the solutions, G is pre-determined with a value of -1.5×10^{-2}. This corresponds to a spherical aluminium particle of a radius $R = 4.4\times10^{-3}$ cm and density $\rho_p = 2.7$ g/cm^3 falling down in water of temperature $T = 45\,^{\circ}\mathrm{C}$ and kinematic viscosity of $\nu_w = 6.05\times10^{-3}$ cm^2/s (such situation may occur, e.g., in the upper layer of nuclear reactor pool vessel). The initial velocity v_0 may be taken to be arbitrary. For other particles, the behaviour of the velocity as a function of time is, in general, qualitatively similar. The solution (10) is shown in Fig. 3 for different values of initial velocity.

It can be observed from Fig. 3 that all curves converge fairly quickly to line 6, independent to any prescribed initial velocity. Here again, particle velocity goes initially to the intermediate asymptotic state described by Eq. (21) and then, asymptotically approach to the final limiting value v_{pt} for infinite time. It is worth

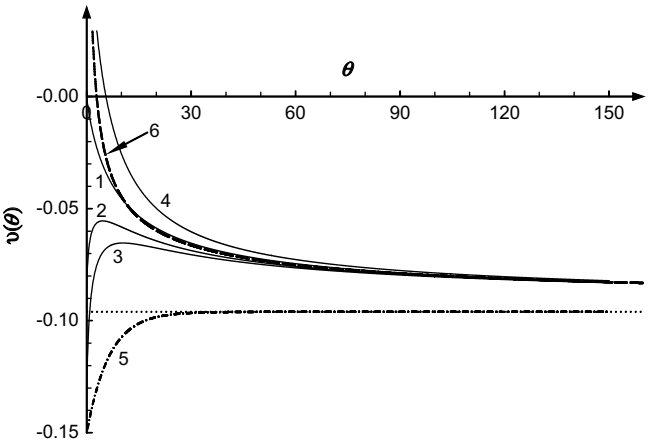

Fig. 3. Velocity versus time in dimensionless variables for a small aluminium particle. Line 1, $\upsilon_0 = 0$; line 2, $\upsilon_0 = \upsilon_{pt} = -9.6 \times 10^{-2}$; line 3, $\upsilon_0 = -0.15$; line 4, $\upsilon_0 = 0.15$; dashed-dotted line 5 shows the velocity relaxation with time when only the SD force is taken into consideration with $\upsilon_0 = -0.15$; and dashed line 6 shows asymptotic dependence (21). Horizontal dotted line shows the terminal velocity.

noting that even when the initial velocity is equivalent to υ_{pt}, the velocity initially deviates from the equilibrium state, decreases by some absolute value with a minimum value at $\theta \approx 4.6$ and then, slowly approaches again the equilibrium state when $\theta \to \infty$. It can also be readily shown that the acceleration of the particle in the vicinity of $\theta = 0_+$ is positive if $\upsilon_0 < 0$ and becomes infinite when $\theta \to 0$. This means that the particle velocity at any negative υ_0 always decreases by absolute value first and then increases and approaches the terminal velocity.

If the BBD force is neglected, the particle velocity due to only SD force exponentially quickly approaches the same equilibrium state in accordance with Eq. (13); the characteristic time of the velocity relaxation is again θ_c as described from above (see, e.g., line 5 in Fig. 3). In this case the velocity does not deviate from the equilibrium state if its initial value is set equal to the terminal velocity. Note that the characteristic time for the particle velocity to achieve the regime described by the intermediate asymptotic is of the same order of magnitude as the relaxation time θ_c.

As the velocity asymptotically approaches to the constant value υ_{pt}, the corresponding traversed path asymptotically varies linearly with time. The dependence of the traversed path on time can be readily obtained from Eqs. (8)–(10) and (12) by simple integration or by the independent solution of Eq. (4) by the Laplace transform method. Corresponding results are presented below for zero initial conditions (the initial particle position due to the translational symmetry can simply be considered zero without loss of generality):

(a) "light particle", $r < 5/8$,

$$\zeta_{Gl}(\theta) = G(r)(2r+1)\left\{2(4-r) - 6\sqrt{\frac{\theta}{\pi}} + \theta + \frac{1}{8\sqrt{5-8r}} \times \left(\left[\left(3-\sqrt{5-8r}\right)^3 e^{\Theta_+}\operatorname{erfc}\left(\sqrt{\Theta_+}\right) - \left(3+\sqrt{5-8r}\right)^3 e^{\Theta_-}\operatorname{erfc}\left(\sqrt{\Theta_-}\right)\right]\right)\right\}; \quad (23)$$

(b) "transient density particle", $r = 5/8$,

$$\zeta_{Gt}(\theta) = \frac{9}{4}G(r)\left[\frac{27}{4} - 9\sqrt{\frac{\theta}{\pi}} + \theta + \left(2\theta - \frac{27}{4}\right)e^{4\theta/9}\operatorname{erfc}\left(\sqrt{\frac{4}{9}\theta}\right)\right] \quad (24)$$

(c) "heavy particle", $r > 5/8$,

$$\zeta_{Gh}(\theta) = G(r)(2r+1)\left\{2(4-r) - 6\sqrt{\frac{\theta}{\pi}} + \theta - 2e^{-a\theta}\left[\frac{9(r-1)}{\sqrt{8r-5}}\sin\left(\theta\sqrt{b}\right) + (4-r)\cos\left(\theta\sqrt{b}\right)\right] + \frac{4r-7}{\sqrt{8r-5}}I\sin(\theta) + 3I\cos(\theta)\right\}. \quad (25)$$

As above, Eq. (25) can be simplified for some special values of r, e.g, for $r = 1$ (in this cases the formula becomes trivial as $G(1) = 0$); 7/4; and 4. In the particular case of $r = 7/4$, when functions $\mathrm{Isin}(\theta, a, b)$ and $\mathrm{Icos}(\theta, a, b)$ reduce to the Fresnel's integrals $S(\theta)$ and $C(\theta)$, Eq. (25) becomes

$$\zeta_{Ghs}(\theta) = \frac{81}{4}G(r)\left\{1 - \frac{4}{3}\sqrt{\frac{\theta}{\pi}} + \frac{2}{9}\theta - \sin\left(\frac{2}{9}\theta\right)\left[1 - 2S\left(\frac{2}{3}\sqrt{\frac{\theta}{\pi}}\right)\right] - \cos\left(\frac{2}{9}\theta\right)\left[1 - 2C\left(\frac{2}{3}\sqrt{\frac{\theta}{\pi}}\right)\right]\right\}. \quad (26)$$

In all above cases (23)–(26), the traversed path is described asymptotically when $\theta \to \infty$ by the following equation:

$$\zeta_{Gas}(\theta) \approx G(r)(2r+1)\left[2(4-r) - 6\sqrt{\frac{\theta}{\pi}} + \theta\right]. \quad (27)$$

Solutions (23)–(26) may also be compared with the solution of Eq. (4) when only the SD force is taken into account and the BBD force is neglected; the exact solution for this case is:

$$\zeta_{GSt}(\theta) = G(r)(2r+1)\left\{\theta + (2r+1)\left[\exp\left(-\frac{\theta}{2r+1}\right) - 1\right]\right\}. \quad (28)$$

The effect of particle initial velocity is additive, as follows from Eq. (6) and the corresponding solutions of Eqs. (8)–(10) and (12). Therefore, if the initial velocity is nonzero, one can simply sum the traversed paths given by the corresponding formulae (15)–(18) and (23)–(26).

3. Motion of a spherical gaseous bubble in a viscous fluid

In this section a similar analysis is performed for a spherical gaseous bubble moving in a viscous fluid; analytical solutions to the equation of motion of a bubble are presented and compared against the results of a solid particle in the previous section.

3.1. Equation of motion and its exact solution

Following Lovalenty and Brady [14], consider a spherical bubble of a radius R travelling in a viscous liquid with an initial velocity V_0 under a buoyancy force. Corresponding equation of motion in the creeping flow regime ($Re \to 0$) is:

$$\left(r + \frac{1}{2}\right)\frac{d^2z}{dt^2} = (1-r)g - \frac{3\nu_f}{R^2} \times \left[\frac{dz}{dt} + 2\int_{-\infty}^{t}\frac{d^2z(\tau)}{d\tau^2}e^{9\nu_f(t-\tau)/R^2}\operatorname{erfc}\sqrt{\frac{9\nu_f}{R^2}(t-\tau)}\,d\tau\right]. \quad (29)$$

Variables from the above equation have the same definitions as in Eq. (1) except for r which now represents gas to liquid density ratio. The equation of motion is applicable not only to gaseous bubbles but also to liquid drops of arbitrary density moving in another fluid with different density with the only restriction that the viscosity of a liquid inside the drop is negligibly small in

comparison with the viscosity of surrounding fluid (an interesting example may be a drop of superfluid moving in a viscous fluid).

If the bubble motion commences at $t=0$ with an initial velocity V_0 so that the total bubble velocity is as above $(\mathrm{d}z/\mathrm{d}t)_{\mathrm{tot}} = \mathrm{H}(t)(\mathrm{d}z/\mathrm{d}t)_{\mathrm{pos}}$ (see Eq. (2)), then an additional term should be included into Eq. (29) due to the effect of Dirac delta-function appearing under the integral:

$$\left(r+\frac{1}{2}\right)\frac{\mathrm{d}^2 z}{\mathrm{d}t^2} = (1-r)g - \frac{3\nu_{\mathrm{f}}}{R^2}\times\left[\frac{\mathrm{d}z}{\mathrm{d}t} + 2V_0 \mathrm{e}^{9\nu_{\mathrm{f}}t/R^2}\mathrm{erfc}\sqrt{\frac{9\nu_{\mathrm{f}}}{R^2}t} + 2\int_{0+}^{t}\frac{\mathrm{d}^2 z(\tau)}{\mathrm{d}\tau^2}\mathrm{e}^{9\nu_{\mathrm{f}}(t-\tau)/R^2}\mathrm{erfc}\sqrt{\frac{9\nu_{\mathrm{f}}}{R^2}(t-\tau)}\,\mathrm{d}\tau\right]. \quad (30)$$

Using normalised variables defined in Eq. (3), Eq. (30) can be rewritten in the dimensionless form as:

$$\frac{\mathrm{d}^2\zeta}{\mathrm{d}\theta^2} = G(r) - \frac{2}{3(1+2r)}\left[\frac{\mathrm{d}\zeta}{\mathrm{d}\theta} + 2\upsilon_0 \mathrm{e}^{\theta}\mathrm{erfc}\sqrt{\theta} + 2\int_{0+}^{\theta}\frac{\mathrm{d}^2\zeta(\vartheta)}{\mathrm{d}\vartheta^2}\mathrm{e}^{\theta-\vartheta}\mathrm{erfc}\sqrt{\theta-\vartheta}\,\mathrm{d}\vartheta\right]. \quad (31)$$

Similar to the particle consideration, the bubble is also assumed to travel in a quiescent fluid. For the sake of simplicity, we further neglect by the gas density inside the bubble and set $r=0$ (for air bubble in water $r \approx 0.0012$).

Eq. (31), similar to Eq. (4), can be solved by the Laplace transform method. After application of the Laplace transformation, the equation for the velocity Laplace image becomes:

$$s\tilde{\upsilon}(s) - \upsilon_0 = \frac{G}{s} - \frac{2}{3}\left[\tilde{\upsilon}(s) + \frac{2s\tilde{\upsilon}(s)}{\sqrt{s}(\sqrt{s}+1)}\right], \quad (32)$$

where $G \equiv G(0)$. Solution to this equation for $\tilde{\upsilon}(s)$ after simple algebra yields:

$$\tilde{\upsilon}(s) = \frac{\upsilon_0\left(s^2+s-(2/3)+(4/3\sqrt{s})\right)}{(s-s_1)\left[(s+\alpha)^2+\beta^2-\alpha^2\right]} + \frac{G}{s}\frac{s^2+s-(2/3)+(4/3\sqrt{s})}{(s-s_1)\left[(s+\alpha)^2+\beta^2-\alpha^2\right]}, \quad (33)$$

where α, β and s_1 are numerical constants; their values are detailed in the Appendix. This formula can be further simplified by expanding the corresponding ratios according to:

$$\tilde{\upsilon}(s) = \upsilon_0 F_1\left\{\frac{1}{s-s_1} + F_2\frac{s+\alpha-F_3}{(s+\alpha)^2+\beta^2-\alpha^2} - \sqrt{\frac{s}{s_1}}\left[\frac{1}{s-s_1} - \frac{(s+\alpha)+s_1-\alpha}{(s+\alpha)^2+\beta^2-\alpha^2}\right]\right\} + \frac{3}{2}\frac{G}{Q_1}\left\{\frac{1}{s-s_1} - \frac{(1+Q_1)(s+\alpha+Q_2)}{(s+\alpha)^2+\beta^2-\alpha^2} + \frac{Q_1}{s} - \sqrt{\frac{s}{s_1}}\left[\frac{1}{s-s_1} + \frac{Q_3(s+\alpha+Q_4)}{(s+\alpha)^2+\beta^2-\alpha^2} - \frac{1+Q_3}{s}\right]\right\}, \quad (34)$$

where F_i and Q_i are also numerical constants, which are formulated in the Appendix.

By application of the inverse Laplace transform, formal solution of Eq. (31) subject to the initial condition can be presented in the form $\upsilon_{\mathrm{b}}(\theta) = \upsilon_{\mathrm{b}\upsilon}(\theta) + \upsilon_{\mathrm{b}G}(\theta)$:

$$\upsilon_{\mathrm{b}\upsilon}(\theta) = -\upsilon_0 F_1\left\{\mathrm{e}^{s_1\theta}\mathrm{erfc}\left(\sqrt{s_1\theta}\right) + \frac{\alpha s_1+\beta^2}{\sqrt{s_1(\beta^2-\alpha^2)}}I\sin\left(\theta,\alpha,\sqrt{\beta^2-\alpha^2}\right) - \sqrt{s_1}I\cos\left(\theta,\alpha,\sqrt{\beta^2-\alpha^2}\right) - F_2\mathrm{e}^{-\alpha\theta}\left[\cos\left(\theta\sqrt{\beta^2-\alpha^2}\right) - \frac{F_3}{\sqrt{\beta^2-\alpha^2}}\sin\left(\theta\sqrt{\beta^2-\alpha^2}\right)\right]\right\}, \quad (35a)$$

$$\upsilon_{\mathrm{b}G}(\theta) = \frac{3}{2}G\left\{1 + \frac{\mathrm{e}^{s_1\theta}}{Q_1}\mathrm{erfc}\left(\sqrt{s_1\theta}\right) - \left(1+\frac{1}{Q_1}\right)\mathrm{e}^{-\alpha\theta}\times\left[\cos\left(\theta\sqrt{\beta^2-\alpha^2}\right) + \frac{Q_2}{\sqrt{\beta^2-\alpha^2}}\sin\left(\theta\sqrt{\beta^2-\alpha^2}\right)\right] + \sqrt{s_1\left(\beta^2-\alpha^2\right)}\left[\frac{\beta^2-\alpha^2+\alpha Q_4}{\alpha-Q_4}I\sin\left(\theta,\alpha,\sqrt{\beta^2-\alpha^2}\right) + I\cos\left(\theta,\alpha,\sqrt{\beta^2-\alpha^2}\right)\right]\right\}. \quad (35b)$$

Similar to the particle motion, the solution also describes two effects: the first part, $\upsilon_{\mathrm{b}\upsilon}(\theta)$, describes the effect of nonzero initial velocity, and the second part, $\upsilon_{\mathrm{b}G}(\theta)$, describes the effect of gravity/buoyancy.

3.2. Bubble versus particle motion in a fluid without gravity

Comparison of the solution for a gaseous bubble is made against with the solution for the rigid particle of negligibly small density ($r=0$), designated here as zero-density rigid particle. It is assumed that both bubble and particle begin to travel with the same initial velocity υ_0 in a viscous fluid without gravity (hence, the buoyancy is also absent). Analysis is therefore concentrated only on the first component of the solutions for the light particle, Eq. (8a), and the bubble, Eq. (35a). Both these solutions are shown in Fig. 4 alongside with the numerical solution of Eq. (4) for the zero-density rigid particle.

The results demonstrate that both theoretical lines for the bubble and light particle solutions converge asymptotically to the same line (dashed line 3 in Fig. 4) described by Eq. (14) with $r=0$. Hence, there is no difference in the behaviour for the zero-density rigid particle and gaseous bubble at large θ; both solutions become indistinguishable when $\theta > 100$. On the other hand, the short-time behaviour is essentially different: particle velocity decays much faster than the bubble velocity; this is illustrated by Fig. 5.

Knowledge of bubble velocity as a function of time allows one to calculate the traversed path by simply integrating Eqs. (35). Corresponding formulae subject to zero initial condition for the bubble instant position is:

$$\zeta_{\mathrm{bub}}(\theta)=\frac{3}{2}v_0\left\{1+\frac{2F_1}{3s_1}\left[e^{s_1\theta}\mathrm{erfc}\left(\sqrt{s_1\theta}\right)+\sqrt{s_1}I\cos\left(\theta,\alpha,\sqrt{\beta^2-\alpha^2}\right)+\frac{(\alpha+s_1)\sqrt{s_1}}{\sqrt{\beta^2-\alpha^2}}I\sin\left(\theta,\alpha,\sqrt{\beta^2-\alpha^2}\right)+\frac{F_2s_1}{\beta^2}(F_3-\alpha)e^{-\alpha\theta}\right]\left(\cos\left(\theta\sqrt{\beta^2-\alpha^2}\right)+\frac{\alpha F_3+\beta^2-\alpha^2}{(F_3-\alpha)\sqrt{\beta^2-\alpha^2}}\sin\left(\theta\sqrt{\beta^2-\alpha^2}\right)\right)\right\}. \tag{36}$$

This solution can be compared with the solution of Eq. (15) for zero-density rigid particle (see Fig. 6).

As illustrated in Fig. 6, both bubble and particle eventually settle to their respective limiting states but the traversed distances are different from each other. The total distance traversed by the bubble is 1.5 times greater than the total distance traversed by the particle at the same initial velocity. This is not entirely surprising as the total drag force experienced by the bubble is 1.5 times smaller than the drag force experienced by the particle. At large θ, both bubble and particle motions reach similar intermediate asymptotic behaviours $\zeta/\zeta_{\max}\sim 1-3/(\pi\theta)^{1/2}$ (cf. Eq. (20)).

3.3. Bubble versus particle motion in a homogeneous fluid under the influence of gravity and buoyancy forces

Consider the bubble motion in a homogeneous viscous fluid when the gravity and buoyancy forces are taken into account. In this case, Eq. (35) shows that, independent of the initial velocity, the bubble velocity asymptotically approaches the terminal velocity $v_{\mathrm{bt}}=3G/2$. This terminal velocity is 1.5 times greater than the terminal velocity of zero-density rigid particle with a slow asymptotic approach $\sim\theta^{-1/2}$ in both cases. Qualitatively, the plots of solutions (35) and (8b) are similar to those shown in Fig. 6.

While the asymptotic approach to the terminal velocity is similar for the bubble and zero-density rigid particle, the velocity behaviour at small time is rather different for them. Early time asymptotic for the rigid particle is linear:

$$v_{\mathrm{lp}}(\theta)\;=\;G\theta, \tag{37}$$

whereas for the bubble velocity the dependence is slightly more complex:

$$v_{\mathrm{bub}}(\theta)\;=\;\frac{3G}{2Q_1}\left\{2\left(\sqrt{\beta^2-\alpha^2}-1\right)\sqrt{\frac{s_1\theta}{\pi}}+[s_1+(1+Q_1)(\alpha-Q_2)]\theta\right\}. \tag{38}$$

The two terms in Eq. (38) are kept because the first term represents the correct velocity behaviour only at very limited time:

$$\theta\ll\theta_{\mathrm{lin}}\equiv\frac{4s_1}{\pi}\left[\frac{\sqrt{\beta^2-\alpha^2}-1}{s_1+(1+Q_1)(\alpha-Q_2)}\right]^2\approx 6.79\times10^{-3}. \tag{39}$$

Comparison of the early-time asymptotics against exact solutions for the bubble and zero-density rigid particle is shown in Fig. 7. Line 1 shows only the first term $\sim\theta^{1/2}$ in the asymptotic formula (38). When both terms are taken into account, there is no difference between the asymptotic and exact solutions in the used time scale.

Another interesting comparison can be made for the bubble and particle velocities as described by equations containing corresponding complete drag forces and equations containing only the SD force. Solution for the particle motion with the SD force only is given by Eq. (13). Analogous solution for the bubble of any density can be readily derived from Eq. (33) with the MID force omitted:

$$v_{\mathrm{St}}(\theta)=v_0\exp\left(-\frac{2}{3}\frac{\theta}{2r+1}\right)+\frac{3}{2}(2r+1)G(r)\left[1-\exp\left(-\frac{2}{3}\frac{\theta}{2r+1}\right)\right]$$

Fig. 8 shows bubble and particle velocities as functions of time described by the formulae with the complete drag forces, Eqs. (35b) and (8b) with $r=0$ correspondingly, and formulae containing the SD force only, Eqs. (39) and (13) correspondingly.

As it is shown in the figure, bubble velocity in the beginning is greater than it is predicted by the approximate formula with the SD force only (cf. lines 1 and 2 in Fig. 8). For $\theta<0.5$ the approximate formula with only the SD force under-predicts the complete solution but it over-predicts the complete solution for $\theta>0.5$. In the case of solid particle, the approximate formula over-predicts the complete solution from the very beginning (cf. lines 3 and 4 in Fig. 8).

The solution for the traversed path can be readily obtained from Eq. (35) by simple integration or by means of the Laplace transform

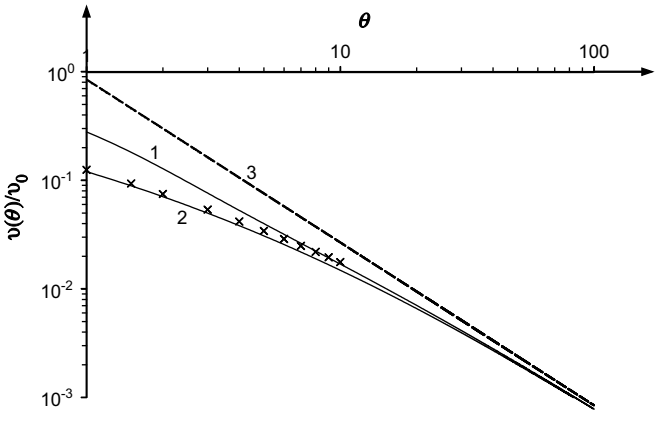

Fig. 4. Normalised velocities of a bubble (line 1) and zero-density rigid particle (line 2) as functions of time in dimensionless variables. Dashed line 3 shows the asymptotic dependence (14) for both these objects. Crosses are results of numerical solution of Eq. (4).

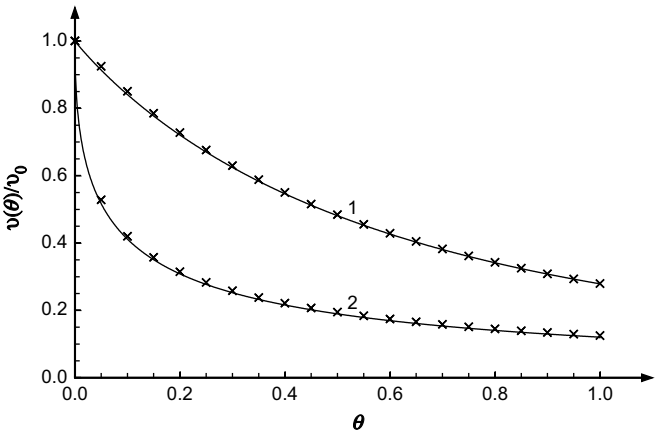

Fig. 5. Early stage of velocity decay with time for a bubble (line 1) and zero-density rigid particle (line 2). Lines are theoretical results and crosses represent numerical data.

of the governing Eq. (31). For the bubble starting motion at the origin from rest, the solution is (cf. Eq. (23)):

$$\zeta_{\mathrm{Gb}}(\theta) = \frac{3}{2}G\left\{\frac{1}{s_1} - \frac{4\alpha+3\beta^2}{2\beta^2} + \frac{\beta^2}{\alpha^2+\beta^2}W\sqrt{\frac{\theta}{\pi}} + \theta - \frac{\sqrt{s_1(\beta^2-\alpha^2)}}{Q_1(\beta^2+\alpha^2)}\left\{\left[\alpha+\beta\left(\frac{\beta^2}{\alpha-Q_4}-\alpha\right)\right]\times I\mathrm{cos}\left(t,\alpha,\sqrt{\beta^2-\alpha^2}\right) - \left[\beta-\alpha\left(\frac{\beta^2}{\alpha-Q_4}-\alpha\right)\right]\times I\mathrm{sin}\left(t,\alpha,\sqrt{\beta^2-\alpha^2}\right)\right\} + \frac{1}{s_1Q_1}\mathrm{e}^{s_1\theta}\mathrm{erfc}\left(\sqrt{s_1\theta}\right) - \frac{1+Q_1}{\beta^2Q_1}\mathrm{e}^{-\alpha\theta}\left[\frac{\beta^2-\alpha(\alpha+Q_2)}{\sqrt{\beta^2-\alpha^2}}\sin\left(\theta\sqrt{\beta^2-\alpha^2}\right) - (\alpha+Q_2)\cos\left(\theta\sqrt{\beta^2-\alpha^2}\right)\right]\right\}, \quad (40)$$

where

$$W = \frac{3s_1(s_1+1)-2}{(s_1+\alpha)^2+\beta^2-\alpha^2}\frac{[\beta s_1+(1+\beta)\alpha]s_1\sqrt{\beta^2-\alpha^2}+\alpha^2+\beta^2}{\sqrt{s_1}},$$

This solution can be compared against the corresponding solution for zero-density particle, Eq. (23) with $r=0$. Another interesting comparison relates to the case when only the SD force is taken into consideration. Corresponding formula for zero-density particle follows from Eq. (28) when $r=0$. Similar expression can be readily derived for a bubble:

$$\zeta_{\mathrm{GStb}}(\theta) = \frac{3}{2}G\left[\theta+\frac{3}{2}(\mathrm{e}^{-2\theta/3}-1)\right] \quad (41)$$

Fig. 9 depicts the comparison of the traversed path for the bubble (line 1) and zero-density particle (line 3). The cases when the MID and BBD forces are omitted and only the SD force is taken into consideration are also shown in the figure (lines 2 and 4 correspondingly). As illustrated in Fig. 9, the formulae based on the SD force provide the same trajectory gradients as the solutions with the complete drag forces; this is not entirely surprising since both the bubble and particle travel asymptotically with their own constant terminal velocities. However, at the early stage of motion, the dynamics of the bubble and particle are different from the models with the consideration of only the SD force. Short-time and long-time asymptotics of the solution for a bubble are:

$$\zeta_{\mathrm{Gbst}}(\theta) \approx \frac{G}{Q_1}2\sqrt{\frac{s_1}{\pi}}\left(\sqrt{\beta^2-\alpha^2}-1\right)\theta^{3/2}\times\left\{1+\frac{3s_1+(1+Q_1)(\alpha-Q_2)}{8\left(\sqrt{\beta^2-\alpha^2}-1\right)}\sqrt{\frac{\pi\theta}{s_1}}+\frac{2}{5}\theta\left[\frac{\beta^2(\beta^2-\alpha^2)-s_1(\alpha-Q_4)}{(\alpha-Q_4)\left(\sqrt{\beta^2-\alpha^2}-1\right)}+\alpha\sqrt{\beta^2-\alpha^2}\right]\right\}, \theta\to 0 \quad (42)$$

$$\zeta_{\mathrm{Gblt}}(\theta) \approx \frac{3}{2}G\left(\frac{1}{s_1}-\frac{4\alpha+3\beta^2}{2\beta^2}+\frac{\beta^2}{\alpha^2+\beta^2}W\sqrt{\frac{\theta}{\pi}}+\theta\right), \quad \theta\to\infty. \quad (43)$$

The last expression can be compared with the corresponding formula for zero-density particle, Eq. (27). The short-time asymptotic for the particle is

$$\zeta_{\mathrm{Gbst}}(\theta) \approx \frac{G}{2}\theta^2\left(1-\frac{16}{5}\sqrt{\frac{\theta}{\pi}}+\frac{8}{3}\theta\right), \quad \theta\to 0. \quad (44)$$

In Fig. 10 short time asymptotics are shown for the bubble and zero-density particle. The bubble with the complete drag force

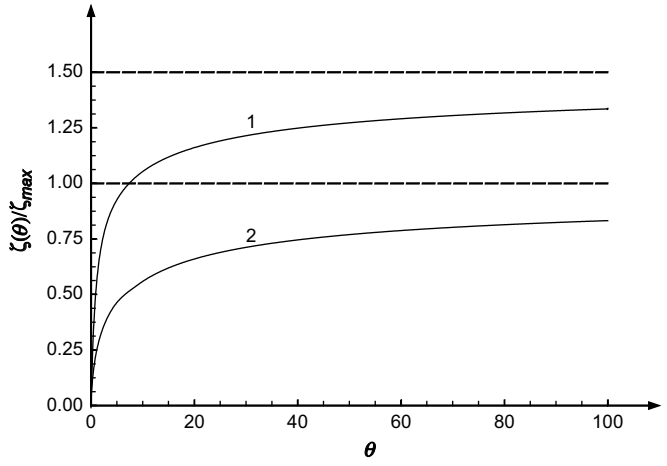

Fig. 6. Comparison of normalised traversed paths as functions of time for the bubble (line 1) and zero-density rigid particle (line 2). Dashed horizontal lines show corresponding limiting values for the traversed paths.

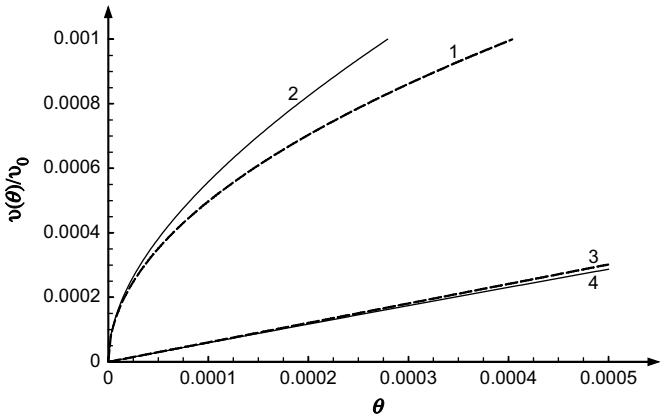

Fig. 7. Behaviour of asymptotic solutions (dashed lines) against exact solutions (solid lines) for the velocities of a bubble (lines 1 and 2) and zero-density rigid particle (lines 3 and 4).

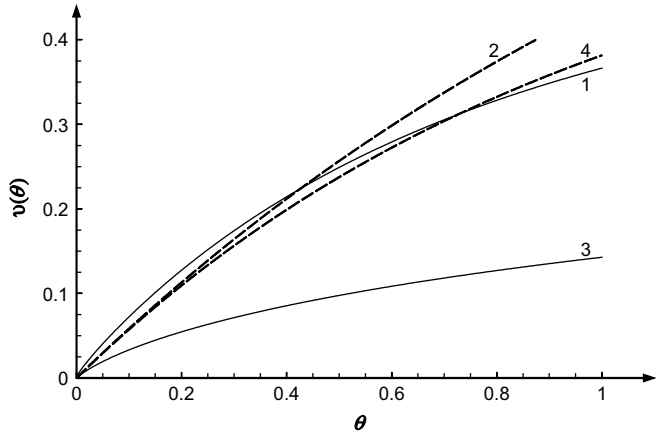

Fig. 8. Velocities of bubble and zero-density solid particle as predicted by the formulae with the complete drag forces (lines 1 and 3 correspondingly) and by approximate formulae containing the SD force only (lines 2 and 4 correspondingly).

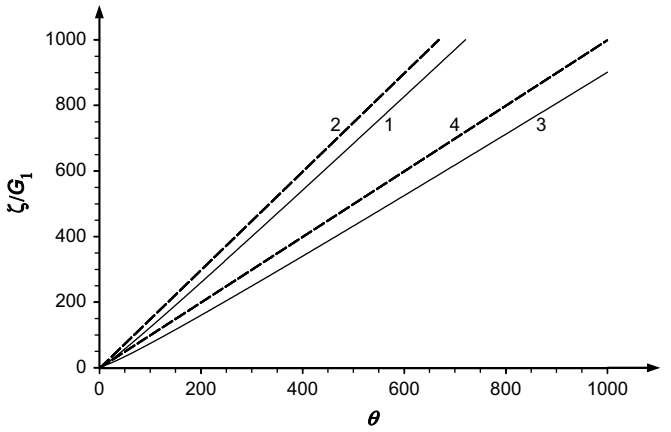

Fig. 9. Normalised traversed paths as functions of time for the: (i) bubble with the complete drag force (line 1) and with the SD force only (line 2) and (ii) zero-density rigid particle with the same forces (lines 3 and 4 correspondingly).

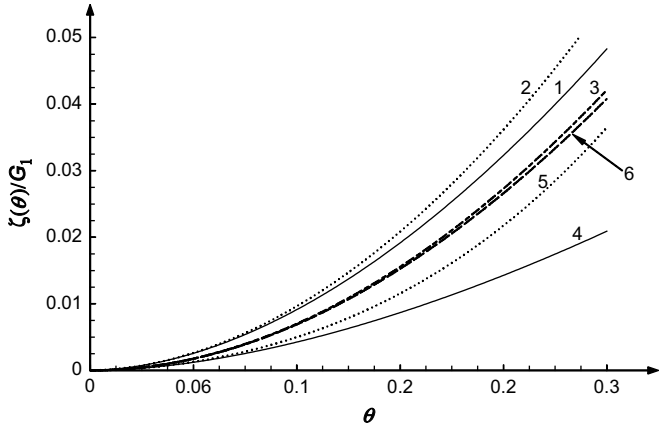

Fig. 10. Short-time asymptotics of normalised traversed paths for the bubble and zero-density rigid particle. Solid line 1, solution for the bubble with the complete drag force; dotted line 2, short-time asymptotic of solution 1; dashed line 3, solution for the bubble with the SD force only; solid line 4, solution for the particle with the complete drag force; dotted line 5, short-time asymptotic of solution 4; dashed line 6, solution for the particle with the SD force only.

initially (until $\theta < 0.5$) travels marginally quicker than it is predicted by the model with only the SD force (cf. lines 1 and 3), whereas for the particle motion the situation is opposite (cf. lines 4 and 6). These dependences are in agreement with the velocity dependences on time presented in Fig. 8 and described above.

Note in the conclusion that in accordance with the creeping flow condition, the terminal velocity for an air bubble in water, v_{bt} must not be greater than 1/9 (see text after Eq. (4)). This leads to the restriction on the bubble radius which in dimensional variables can be presented as:

$$R_{bub} \leq \sqrt[3]{\frac{3\nu_f^2}{g}} = 5.5 \times 10^{-3} \text{ cm}. \tag{45}$$

4. Conclusion

A comparative analysis of exact solutions to the equations of motion for a solid particle and a gaseous bubble is performed. In essence, the equations of motion are the Newtonian equations which include, in general, the Stokes drag force and memory-integral drag force. Expressions for these forces are different for solid particles and bubbles. Some common as well as different features in the dynamics of these two inclusions are revealed. In particular, it is shown that the dynamics of a solid particle of negligibly small density is different from the bubble dynamics. Thus, for instance, if both these inclusions commence their motion with the same initial velocity in a fluid without gravity, they eventually come to the rest covering a finite but different distances. The path traversed by the bubble is 1.5 times greater than the path traversed by a solid particle of the same radius. In the presence of gravity, both the particle and bubble asymptotically travel with their respective terminal velocities; and the bubble terminal velocity is again 1.5 times greater than the terminal velocity of a solid particle of negligibly small density in comparison with the fluid density.

If external conditions remain unchanged, so that the particle and bubble asymptotically approach to their respective relaxing motion, their long-time dynamics can be satisfactorily described by the much simpler model which accounts for only the Stokes drag force (with different numerical coefficients for the particle and bubble, however [2,12]). Meanwhile, for the description of the early-stage dynamics, i.e. when the displacement varies from units to several hundreds of particle/bubble radii, the simplified model is not valid and the complete drag force considerations need to be taken into account.

On the basis of exact analytical solutions derived in this paper, we confirmed that the MID force with the integral kernels relevant to solid particles and zero viscosity drops (including gaseous bubbles at certain approximation) is positive and monotonically decreasing (i.e., it is a dissipative force), at least in the simple cases considered in this paper (see also [8,21]). Meanwhile, Galindo and Gerbeth [8] revealed that the MID force can be negative at some relationship between the density ratio of internal to external liquid and corresponding viscosity ratio. This implies that in such cases the MID force may act as an acceleration force pumping a kinetic energy into the inclusion, at least momentarily [11]. In other words, the MID force, probably, may provide a way of the kinetic energy transformation from an external flow to the inclusion. If it is indeed the case, it would be of interest to investigate a condition when such transformation is possible and the effectiveness of the transformation depending on the characteristics of external flow and relationship between the density and viscosity ratios.

As aforementioned in Section 1, applicability of the results obtained in this paper is based on two basic assumptions. Firstly, on the creeping flow approximation, which formally presumes vanishingly small Reynolds numbers ($Re \to 0$). However, in practice this restriction is not so strong and can be extended up to $Re \lesssim 1$ (see, e.g. Fig. 4.9.2 in book [2] and the concomitant text there). Secondly, as was shown by Lovalenty and Brady [14], there is a formal restriction on the time interval, $t < t_{lim} \equiv \rho R^2/\mu$, when the MID force can be described by the simplest expressions used in this paper. For a solid or gaseous inclusion of a radius $R = 3$ mm, the upper limit of the time interval is $t_{lim} \approx 9$ s and this time decreases quadratically with the inclusion radius R. From the physical point of view this restriction is determined by the condition that the vorticity generated at the inclusion surface is confined within the Stokes region [12] of the moving body and not advected yet into the wake behind the body. Afterwards, when the vorticity is advected into the wake, the flow adapts more quickly to the changes in the particle velocity, resulting in a sharper decay of the MID force. This means that the transitional dynamics of an inclusion in a quiescent fluid relax to the stationary motion even faster than it is predicted by the solutions obtained here. In the stationary regime an inclusion moves with the terminal velocity which is characterised by the balance of driving (gravitational) force and SD force only. Hence, if the relaxation to the terminal velocity occurs within the time interval $t < t_{lim}$, then the solutions derived in this paper describes this process absolutely correctly. Otherwise, beyond this time interval the solutions obtained describe the process of relaxation qualitatively correctly although quantitatively the relaxation occurs faster.

Appendix. Coefficients in the solution describing bubble motion in viscous fluid

For a gaseous bubble of negligibly small density and viscosity in comparison with the density and viscosity of a surrounding fluid, the coefficients in the solutions (37)–(39) are simply numbers that are irrational however and rather long. Their exact (in terms of surds) and approximate numerical values are:

$$s_1 = \frac{1}{3}\left(q^{1/3} + q^{-1/3}\right) - 1 \approx 0.142676, \tag{A1}$$

where $q = 15 + 4\sqrt{14} \approx 29.96663$.

$$\alpha = 2\,\frac{7q^{2/3} - 2q^{1/3} - 2q}{\left(q^{2/3} - 3q^{1/3} + 1\right)^2} \approx 1.571338;$$

$$\beta = \sqrt{\frac{4}{3}\,\frac{q^{1/3}}{q^{2/3} - 3q^{1/3} + 1}} \approx 1.764951 \tag{A2}$$

$$F_1 = -\frac{4}{3}\,\frac{\sqrt{s_1}}{(s_1+\alpha)^2 + \beta^2 - \alpha^2} \approx -0.140531;$$

$$F_2 = \frac{(2\alpha - 1)s_1 + \beta^2 + (2/3)}{(s_1 + 1/2)^2 - (11/12)} \approx -8.115875;$$

$$F_3 = \frac{8}{3}\,\frac{361q^{5/3} - 51q^{4/3} - 3328q - 2q^{1/3} + 111}{369q^{5/3} - 1060q^{4/3} - 6857q - 43q^{1/3} + 230} \approx 0.164651. \tag{A3}$$

$$Q_1 = \frac{2}{\beta^2}\,\frac{(s_1+\alpha)^2 + \beta^2 - \alpha^2}{3s_1(s_1+1) - 2} \approx -1.522901;$$

$$Q_2 = \frac{\left[3\beta^2(1-\alpha) + 2\alpha\right]s_1 + 4\alpha^2 - \beta^2\left(3\beta^2 - 3\alpha + 2\right)}{\left(3\beta^2 + 2\right)s_1 + 3\beta^2 + 4\alpha} \approx -0.643122;$$

$$Q_3 = \frac{s_1(s_1 + 2\alpha)}{\beta^2} \approx 0.150477;$$

$$Q_4 = \frac{\alpha s_1 + 2\alpha^2 - \beta^2}{s_1 + 2\alpha} \approx 0.623174. \tag{A4}$$

References

[1] G.I. Barenblatt, Scaling, Cambridge University Press, Cambridge, 2003.
[2] J.K. Batchelor, An Introduction to Fluid Dynamics, Cambridge University Press, Cambridge, 1970.
[3] F. Candelier, J.R. Angilella, M. Souhar, On the effect of the Boussinesq–Basset force on the radial migration of Stokes particle in a vortex, Phys. Fluids 16 (2004) 1765–1776.
[4] F. Candelier, J.R. Angilella, M. Souhar, On the effect of inertia and history forces on the slow motion of a spherical solid or gaseous inclusion in a solid-body rotation flow, J. Fluid Mech. 545 (2005) 113–139.
[5] R. Clift, J. Grace, M.E. Weber, Bubbles, Drops, and Particles, Dover Publ. Inc., Mineola, New York, 2005.
[6] C.F.M. Coimbra, M.H. Kobayashi, On the viscous motion of a small particle in a rotating cylinder, J. Fluid Mech. 469 (2002) 257.
[7] O.A. Druzhinin, L.A. Ostrovsky, The influence of Basset force on particle dynamics in two-dimensional flows, Physica D 76 (1994) 34–43.
[8] V. Galindo, G. Gerbeth, A note on the force on an accelerating spherical drop at low-Reynolds number, Phys. Fluids A 5 (1993) 3290–3292.
[9] V.A. Gorodtsov, Creeping motion of a drop in a viscous fluid, J. Appl. Mech. Tech. Phys. 16 (1975) 865–868 (Engl. transl. from the Russian journal Zhurn. Prikl. Mekh. Tekh. Fiz. 6 (1975) 32–37.
[10] S. Kim, S.J. Karrila, Microhydrodynamics: Principles and Selected Applications, Butterworth–Heinemann, Boston, 1991, (second unabridged republication: Dover Publ. Inc., Mineola,New York, 2005)154–162.
[11] M.H. Kobayashi, C.F.M. Coimbra, On the stability of the Maxey–Riley equation in nonuniform linear flows, Phys. Fluids 17 (2005) 113301, 14 pp.
[12] L.D. Landau, E.M. Lifshitz, in: Hydrodynamics, fourth ed. Nauka, Moscow, 1988 (Engl. Transl.: Fluid Mechanics, Pergamon Press, Oxford, 1993).
[13] D. Legendre, J. Magnaudet, A note on the lift force on a spherical bubble or drop in a low-Reynolds-number shear flow, Phys. Fluids 9 (1997) 3572–3574.
[14] P.M. Lovalenti, J.F. Brady, The force on a bubble, drop, or particle in arbitrary time-dependent motion at small Reynolds number, Phys. Fluids A 5 (1993) 2104–2116.
[15] E.E. Michaelides, Hydrodynamic force and heat/mass transfer from particles, bubbles, and drops – the Freeman Scholar lecture, J. Fluid Eng 125 (2003) 209–238.
[16] N.V. Parshikova, The drag force on a drop in a viscous nonhomogeneous non-stationary flow, Vestnik Moskovskogo Universiteta, Ser. 1: Mat., Mekh 4 (1982) 63–67 (in Russian).
[17] F. Sy, J.W. Taunton, E.N. Lightfoot, Transient creeping flow around spheres, AIChE 16 (1970) 386–391.
[18] P.J. Thomas, On the influence of the Basset history force on the motion of a particle through a fluid, Phys. Fluids A 4 (1992) 2090–2093.
[19] P.J. Thomas, A numerical study of the influence of the Basset force on the statistics of LDV velocity data sampled in a region with a large spatial velocity gradient, Experiments in Fluids 23 (1997) 48–53.
[20] E.W. Weisstein, in: CRC Concise Encyclopedia of Mathematics, second ed. Chapman & Hall/CRC, Boca Raton, 2003 see also: http://functions.wolfram.com/.
[21] S.M. Yang, L.G. Leal, A note on memory-integral contributions to the force on an accelerating spherical drop at low Reynolds number, Phys. Fluids A 3 (1991) 1822–1824.